

# Co-Crystals of Sulfamethazine with Some Carboxylic Acids and Amides: Co-Former Assisted Tautomerism in an Active Pharmaceutical Ingredient and Hydrogen Bond Competition Study

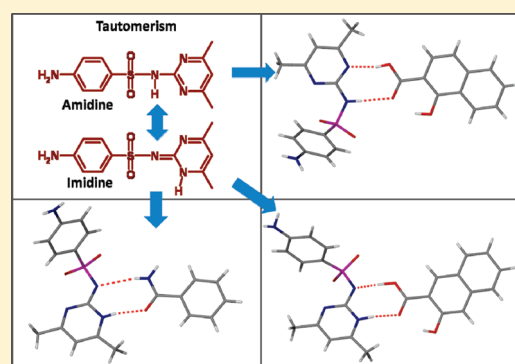
Published as part of a virtual special issue on Structural Chemistry in India: Emerging Themes

Soumyajit Ghosh, Partha Pratim Bag, and C. Malla Reddy\*

Department of Chemical Sciences, Indian Institute of Science Education and Research, Kolkata, West Bengal 741252, India

**S** Supporting Information

**ABSTRACT:** Ten new co-crystals of an antibacterial drug sulfamethazine (SFZ) with various carboxylic acid and amide co-formers have been synthesized. These new forms are characterized by single crystal X-ray diffraction, infrared spectroscopy, differential scanning calorimetry (DSC), and thermogravimetric analysis (TGA). Crystal structures with 4-hydroxybenzoic acid (HBA), 2,4-dihydroxybenzoic acid (DHB), 3,4-dichlorobenzoic acid (DCB), sorbic acid (SOR), fumaric acid (FUM), 1-hydroxy-2-naphthoic acid (1HNA), benzamide (BEN), picolinamide (PIC), 4-hydroxybenzamide (HBEN), and 3-hydroxy-2-naphthoic acid (3HNA) are determined. The SFZ molecule displays co-former assisted amidine to imidine tautomerism in the co-crystals in that the sulfonamide NH proton moves to one of the pyrimidine N atoms. In all the cases, the SFZ forms a robust hydrogen bonded synthon with a carboxylic acid (amidine<sub>(SFZ)</sub>···acid/imidine<sub>(SFZ)</sub>···acid) or amide (imidine<sub>(SFZ)</sub>···amide) group from the co-former. The SFZ molecule, in all the carboxylic acid and



exists in the imidine tautomeric form while it exists in amidine tautomeric form in the rest of the acid co-crystals. Density functional theory (DFT) calculations revealed that the amidine tautomer in free SFZ is much more stable than its imidine tautomeric form, while when it is hydrogen bonded to the co-formers via acid or amide groups, the difference is greatly minimized. But the synthon formation between the stable amidine<sub>(SFZ)</sub> and amide co-former is sterically hindered; hence the SFZ tautomerizes itself to the imidine<sub>(SFZ)</sub> form to facilitate the formation of a robust imidine<sub>(SFZ)</sub>···amide synthon in all the amide based co-crystals in this study. Solubility properties of some of the new co-crystal forms are also studied. The crystal structures are analyzed in the context of hydrogen bond competition between various acceptors and donors, in the presence of other competing functional groups, in the active pharmaceutical ingredient (API) co-crystals.

## INTRODUCTION

The crystal engineering approach has generally been a successful design strategy for obtaining new co-crystal forms of active pharmaceutical ingredients (APIs) for desired physico-chemical properties without affecting the pharmacological behavior of the drug.<sup>1,2</sup> In recent times, this has been utilized successfully to modify the API stability, solubility, bioavailability, mechanical properties, etc.<sup>3</sup> Particularly, crystal engineering, based on the synthon approach is an effective route that provides the basis for the selection of co-formers to achieve predetermined structures, thus properties, with a higher success rate.<sup>4</sup> Hence, it is important to understand the precise role of functional groups, especially in the presence of other competing functionalities.<sup>5</sup> Sulfa drugs have been interesting in this context and studied to understand the hydrogen bond preferences of the strong hydrogen bonding groups such as SO<sub>2</sub>, NH<sub>(sulfonamide)</sub>, NH<sub>2</sub>, etc. present on them.<sup>5d</sup>

Sulfamethazine (SFZ; Scheme 1) is a sulfonamide drug, sometimes known as sulfadimidine or sulfadimethylpyridine, that is used to treat a variety of bacterial diseases in human and veterinary

medicine.<sup>6</sup> Sulfamethazine is an anti-infective agent that has a spectrum of antimicrobial actions similar to that of other sulfa-drugs.<sup>7</sup> Sulfamethazine is used for veterinary purposes to treat a variety of infections, as well as being utilized in the management of diseases in herds. It is also used to treat urinary tract infection, chlamydia, rheumatoid fever, toxoplasmosis, and malaria in humans. Sulfamethazine is primarily used as an antibacterial drug and growth promoter in food animals, such as cattle, pigs, and poultry. The usage of SFZ in high dosages has side effects, such as hypersensitivity, photosensitivity, vomiting, etc.

Sulfamethazine has two types of donors (amine NH<sub>2</sub>, and a sulfonamide NH) that in total bear three acidic protons. And, there are three types of acceptors, namely, two sulfoxy O atoms, one amine N, and two pyrimidine N atoms that are capable of forming hydrogen bonds in the co-crystal. Sulfamethazine is

**Received:** March 16, 2011

**Revised:** May 7, 2011

**Published:** June 01, 2011

known to form co-crystals with aspirin, benzoic acid, 2,4-dinitrobenzoic acid, trimethoprim, 4-aminosalicylic acid, theophylline, etc.<sup>8</sup> In this article, we report a series of new co-crystals of SFZ with various co-formers achieved by a co-crystal screening process (Scheme 1). The present series of co-crystals also gave us a chance to study the hydrogen bonding preferences of the acceptor and donor groups present on both SFZ and the co-formers.

## EXPERIMENTAL SECTION

**Materials.** Sulfamethazine drug and all co-crystal formers were purchased from Sigma-Aldrich. Commercially available solvents were used as received without further purification.

**Single Crystal Preparation.** Sulfamethazine drug and co-crystal former in a definite stoichiometric ratio were subjected to grinding with an addition of a few drops of acetonitrile solvent using an agate mortar and pestle for about 10 min. After grinding, the mixture was transferred to a 10 mL conical flask followed by addition of acetonitrile. The suspension was heated until a clear solution was obtained. The resulting mixture was boiled for 10 min before being filtered into a fresh conical flask. The filtrate was left to evaporate slowly at ambient conditions. The single crystals suitable for X-ray diffraction studies were obtained in 4–6 days. Similarly, the co-crystals could also be prepared from acetone, methanol, and ethanol solvents.

**Scheme 1. Molecular Structures of the Compounds Used for Co-Crystallization in This Study**

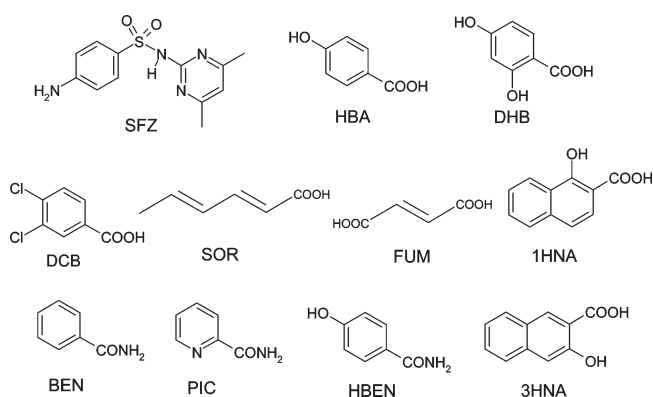


**Table 1. New Sulfamethazine Co-Crystals with Various Carboxylic Acid and Amide Co-Formers and Corresponding Melting Points**

co-crystal structure code	co-former name (code)	co-crystal, mp (°C) $T_{max}$ from DSC	co-former, mp (°C) <sup>a</sup>
SFZ/HBA	4-hydroxybenzoic acid (HBA)	220.7	214–215
SFZ/DHB	2,4-dihydroxybenzoic acid (DHB)	200.7	225–227
SFZ/DCB	3,4-dichlorobenzoic acid (DCB)	191.5	206
SFZ/SOR	sorbic acid (SOR)	169.6	132–135
SFZ/FUM/ACN	fumaric acid (FUM)	199.0	299–300
SFZ/1HNA	1-hydroxy-2-naphthoic acid (1HNA)	190.2	195–200
SFZ/BEN	benzamide (BEN)	185.4	130–133
SFZ/PIC	picolinamide (PIC)	163.7	110
SFZ/HBEN-T <sup>b</sup>	4-hydroxybenzamide (HBEN)	180.0	161–162
SFZ/HBEN-M <sup>c</sup>		175.2	
SFZ/3HNA	3-hydroxy-2-naphthoic acid (3HNA)	199.2	218–221

<sup>a</sup> Melting point values as reported in Sigma-Aldrich chemical catalog. <sup>b</sup> T = triclinic. <sup>c</sup> M = monoclinic.

**NMR.** <sup>1</sup>H nuclear magnetic resonance (NMR) analysis of single crystals (2–3) was performed on a JEOL 400 MHz NMR in DMSO-*d*<sub>6</sub> at 25 °C to confirm the API to co-former ratio.

**Powder X-ray Diffraction (PXRD).** The PXRD patterns were collected on a Rigaku SmartLab with a Cu K $\alpha$  radiation (1.540 Å). The tube voltage and amperage were set at 40 kV and 50 mA, respectively. Each sample was scanned between 10 and 90° 2 $\theta$  with a step size of 0.02° (Figure S11, Supporting Information). The instrument was previously calibrated using a silicon standard.

**Crystallography.** Co-crystals of sulfamethazine were individually mounted on a glass pip. Intensity data were collected on a Bruker's KAPPA APEX II CCD Duo system with graphite-monochromatic Mo K $\alpha$  radiation ( $\lambda = 0.71073$  Å). The data were collected at 296 K temperature for all the co-crystals, except SFZ/3HNA, SFZ/1HNA, and SFZ/FUM/ACN which were collected at 100 K. Data reduction was performed using Bruker SAINT software.<sup>9a</sup> Crystal structures were solved by direct methods using SHELXL-97 and refined by full-matrix least-squares on  $F^2$  with anisotropic displacement parameters for non-H atoms using SHELXL-97.<sup>9b</sup> Hydrogen atoms associated with carbon atoms were fixed in geometrically constrained positions. Hydrogen atoms associated with oxygen and nitrogen atoms were included in the located positions. Structure graphics shown in the figures were created using the X-Seed software package version 2.0.<sup>10</sup>

**Melting Point.** Melting points of co-crystals and the individual co-formers were measured using a digital melting point apparatus, SECOR INDIA.

**Differential Scanning Calorimetry (DSC).** DSC was conducted on a Mettler-Toledo DSI1 STAR<sup>e</sup> instrument. Accurately weighed samples (2–3 mg) were placed in hermetically sealed aluminum crucibles (40  $\mu$ L) and scanned from 30 to 300 °C at a heating rate of 5 °C/min under a dry nitrogen atmosphere (flow rate 80 mL/min). The data were managed by STAR<sup>e</sup> software.

**Thermogravimetric Analysis (TGA).** TGA was performed on a Mettler-Toledo TGA/SDTA 851<sup>e</sup> instrument. Approximately 10–15 mg of the sample was added to an aluminum crucible and heated from 30 to 500 °C at a rate of 10 °C/min under continuous nitrogen purge.

**IR Spectroscopy.** Transmission infrared spectra of the solids were obtained using a Fourier-transform infrared spectrometer (PerkinElmer 502). KBr samples (2 mg in 20 mg of KBr) were prepared and 10 scans were collected at 4  $\text{cm}^{-1}$  resolution for each sample. The spectra were measured over the range of 4000–400  $\text{cm}^{-1}$ .

**Solubility Studies.** The solubility studies for powder samples of single component SFZ and its co-crystals with SOR, FUM, 1HNA, BEN, PIC, and 3HNA were performed according to the literature procedures.<sup>11</sup>

Excess amounts (~ 80 mg) of the samples were suspended in 10 mL of water in a 25 mL round-bottom flask (rbf) and closed with a glass stopper. These rbf were kept in a cupboard for 72 h at ~23 °C and were stirred at 500 rpm using a magnetic stirrer. After 72 h, the suspensions were filtered through a filter paper (90 mm). The filtered aliquots were sufficiently diluted and the absorbance was measured in the range of 200–800 nm. Finally, the concentration of SFZ after 72 h (apparent aqueous solubility) in each sample was determined from the previously made standard graph. A standard graph was made by measuring the absorbance of varied concentrations of SFZ in water using a UV spectrophotometer (HITACHI U-4100).

**Computational Details.** Geometry optimizations were performed with Gaussian 03<sup>12</sup> using the B3LYP method<sup>13</sup> with the 6-31G(d) basis set,<sup>14</sup> followed by single point energy calculation at the 6-311++G (2df, 2p) level, in a density functional theory (DFT) type calculation. The initial atomic coordinates for all the molecules were taken from the crystal structures.

## RESULTS AND DISCUSSION

Ten new co-crystals of SFZ with various carboxylic acid and amide co-formers were synthesized by the slow evaporation crystallization method (Table 1). These new solid phases were characterized by PXRD, IR spectroscopy, DSC and TGA. Single crystal X-ray structures with 4-hydroxybenzoic acid (HBA), 2,4-dihydroxybenzoic acid (DHB), 3,4-dichlorobenzoic acid (DCB), sorbic acid (SOR), fumaric acid (FUM), 1-hydroxy-2-naphthoic acid (1HNA), benzamide (BEN), picolinamide (PIC), 4-hydroxybenzamide (HBEN), and 3-hydroxy-2-naphthoic acid (3HNA) were determined. Crystal structure analysis was done to rationalize the hydrogen bonding preferences of acceptors and donors in the presence of other competing functional groups. A comparison of experimental PXRD patterns with those calculated from corresponding single crystal data and DSC established the phase purity of the solids. The same batches of samples were used for IR spectroscopy and solubility studies. Crystallographic data are listed in Table 2. Hydrogen bond table (Table S1, Supporting Information) and the ORTEP diagrams for all the co-crystals are included in the Supporting Information (Figures S1–S10).

**Sulfamethazine/4-Hydroxybenzoic Acid (1:1), (SFZ/HBA).** The co-crystal SFZ/HBA crystallizes in the triclinic  $P\bar{1}$  space group with one molecule of each SFZ and HBA in the asymmetric unit. The SFZ molecule adopts a V-shape conformation in that the two aromatic rings are twisted to take a propeller shape. The co-former, HBA molecule, possesses two strong hydrogen bonding functional groups: a carboxylic acid and a hydroxyl group at the para position on its phenyl ring. In the structure, the SFZ molecule exists in the imidine tautomeric form that results from the transfer of proton from sulfonamide NH to the pyrimidine ring N as shown in Scheme 3. Hence, in this case, the SFZ molecule offers the imidine site for binding with the HBA acid functional group via synthon 2 (see Scheme 2; O(4)–H(4)···N(3);  $d/\text{Å}$ ,  $\theta/^\circ$ ; 2.01 (4) Å, 169(5)°; N(1)–H(1)···O(3); 1.79(3) Å, 177.7(16)°). The robust synthon 2 holds the SFZ pyrimidine ring and HBA phenyl ring in the same plane, which is also the case in all the co-crystals in this study. The HBA *p*-hydroxyl group interacts with the amine group from an adjacent SFZ molecule via O(5)–H(5)···N(4) (synthon 7; 2.13(4) Å, 163(4)°) that eventually leads to a tetramer shown in Figure 1a. One of the two amine hydrogens forms N(4)–H(4B)···O(1) (2.22(3) Å, 165(3)°) hydrogen bond with the sulfoxy O-atom to join the adjacent tetramers to form a ladder (with steps on either side as seen in Figure 1b) along the *a*-axis,

while the second hydrogen of the NH<sub>2</sub> group forms N(4)–H(4A)···N(2) (2.59(3) Å, 168(2)°) hydrogen bond with the pyrimidine ring of SFZ from another adjacent tetramer. The HBA phenyl rings stack over the SFZ pyrimidine rings from adjacent ladders. In addition, there are several weak interactions such as C–H···O to  $\pi$ ··· $\pi$  between the ladders. All the good acceptors and donors are fully utilized in this structure.

**Sulfamethazine/2,4-Dihydroxybenzoic acid (1:1), (SFZ/DHB).** The co-crystal, SFZ/DHB, crystallizes in triclinic  $P\bar{1}$  space group with one molecule of each SFZ and DHB in the asymmetric unit. The unit cell parameters of the co-crystal SFZ/DHB suggest that it is isostructural to SFZ/HBA (Table 1). However, surprisingly, the SFZ molecule exists in the amidine tautomeric form but not in the imidine tautomeric form as in SFZ/HBA. Barring this difference, the rest of the packing is very similar (Figure 2). In the structure, the extra *ortho*-OH group on DHB does not interfere in the overall packing as it primarily involves an intramolecular hydrogen bond (O(5)–H(5A)···O(4); 1.68(5) Å, 151(4)°) with the carbonyl O atom.

**Sulfamethazine/3,4-Dichlorobenzoic Acid (1:1), (SFZ/DCB).** The SFZ and DCB molecules co-crystallize in monoclinic  $P2_1/n$  space group with one molecule of each in the asymmetric unit. The SFZ molecule adopts an L-shape conformation in that the two aromatic ring planes are face-to-face. In the co-crystal, the carboxylic acid group from DCB forms synthon 1 with the SFZ molecule. The packing in this structure is mostly dominated by synthon 5 in that the N–H···O hydrogen bonds are formed between the SO<sub>2</sub> and NH<sub>2</sub> groups, both from SFZ, leading to the formation of a polar two-dimensional (2D) square grid network parallel to the (010) plane (Figure 3). The pyrimidine rings lie below and above nearly perpendicular to the plane of the 2D network. The adjacent polar layers are packed in an antiparallel fashion so that the  $\pi$ ··· $\pi$  interactions are optimized by the stacking of pyrimidine and co-former rings from the opposite layers.

**Sulfamethazine/Sorbic Acid (1:1), (SFZ/SOR).** Sorbic acid is an unsaturated carboxylic acid used as a food preservative. The co-crystal crystallizes in monoclinic  $P2_1/c$  space group in that the SOR molecule adopts planar conformation. As expected, the naturally occurring co-former, SOR, forms synthon 1 with SFZ in the co-crystal. The amine group uses its two protons to form two N(4)–H(4A)···O(1) (2.29(4) Å, 135(4)°) and N(4)–H(5A)···O(3) (2.29(4) Å, 164(3)°) hydrogen bonds, one with SO<sub>2</sub> group (synthon 5) and the second with the carbonyl O-atom of an adjacent SOR molecule. This eventually leads to the formation of a 2D-sheet parallel to the (100) in that pyrimidine rings of the alternate SFZ molecules protrude out almost perpendicularly from either side of the 2D sheet as shown in Figure 4. The SFZ pyrimidine rings and SOR unsaturated chains (that form synthon 1) are packed antiparallely over the other similar pairs from adjacent 2D sheets to interdigitate the structure via  $\pi$ ··· $\pi$  interactions.

**Sulfamethazine/Fumaric Acid/Acetonitrile, (2:1:1) (SFZ/FUM/ACN).** It crystallizes in the orthorhombic *Pbcn* space group with two SFZ, one FUM, and a disordered acetonitrile molecule in the asymmetric unit. This is the only co-crystal solvate in the present series and is interesting in the context of crystal packing analysis. In the crystal structure, the dicarboxylic acid, FUM, binds with two SFZ molecules via synthon 1 to form a trimer. The adjacent trimers are linked via synthon 5 (N(4)–H(4A)···O(3); 2.14(2) Å, 164.6(19)° and N(4)–H(4B)···O(2); 2.20(2) Å, 156.1(17)°) involving the amine (NH<sub>2</sub>) and SO<sub>2</sub> groups from

Table 2. Crystallographic Data and Structure Refinement Parameters of SFZ Co-Crystals

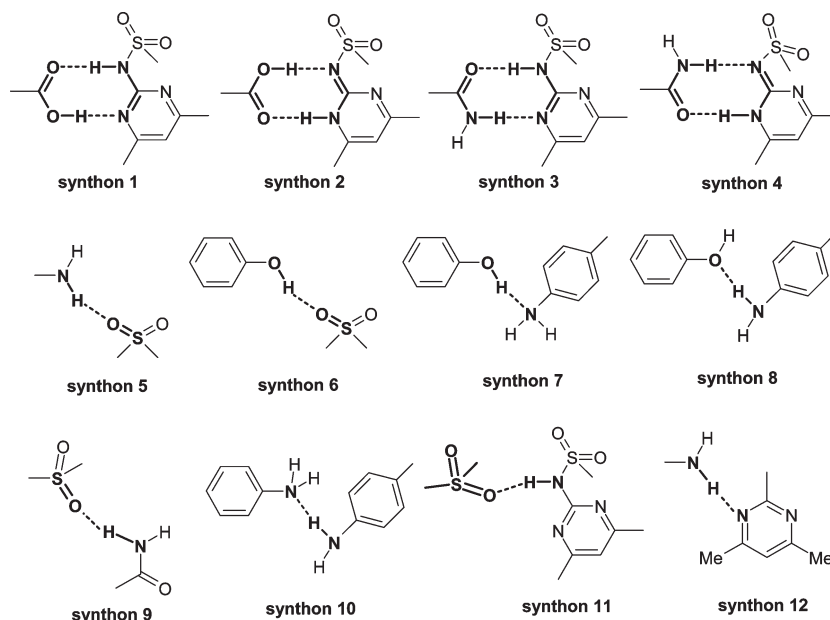
	SFZ/HBA	SFZ/DHB	SFZ/DCB	SFZ/SOR	SFZ/FUM/ ACN	SFZ/1HNA
chemical formula	C <sub>12</sub> H <sub>14</sub> N <sub>4</sub> O <sub>2</sub> S, C <sub>7</sub> H <sub>6</sub> O <sub>3</sub>	C <sub>12</sub> H <sub>14</sub> N <sub>4</sub> O <sub>2</sub> S, C <sub>7</sub> H <sub>6</sub> O <sub>4</sub>	C <sub>12</sub> H <sub>14</sub> N <sub>4</sub> O <sub>2</sub> S, C <sub>7</sub> H <sub>4</sub> Cl <sub>2</sub> O <sub>2</sub>	C <sub>12</sub> H <sub>14</sub> N <sub>4</sub> O <sub>2</sub> S, C <sub>6</sub> H <sub>8</sub> O <sub>2</sub>	2(C <sub>12</sub> H <sub>14</sub> N <sub>4</sub> O <sub>2</sub> S), C <sub>4</sub> H <sub>4</sub> O <sub>4</sub> , C <sub>2</sub> H <sub>3</sub> N	C <sub>12</sub> H <sub>14</sub> N <sub>4</sub> O <sub>2</sub> S, C <sub>11</sub> H <sub>8</sub> O <sub>3</sub>
formula weight	416.45	432.45	469.33	390.46	713.79	466.51
cryst sys	triclinic	triclinic	monoclinic	monoclinic	orthorhombic	triclinic
space group	<i>P</i> $\bar{1}$	<i>P</i> $\bar{1}$	<i>P</i> 2 <sub>1</sub> / <i>n</i>	<i>P</i> 2 <sub>1</sub> / <i>c</i>	<i>Pbca</i>	<i>P</i> $\bar{1}$
<i>a</i> (Å)	8.0060(5)	7.9671(3)	8.1070(4)	8.6932(4)	11.4148(7)	12.1076(8)
<i>b</i> (Å)	9.3913(5)	9.4629(4)	17.5194(8)	17.0624(7)	20.1672(12)	13.5903(9)
<i>c</i> (Å)	13.4786(8)	13.9432(6)	14.7732(7)	14.2695(6)	14.8653(9)	14.7508(10)
$\alpha$ (°)	74.611(3)	73.662(2)	90	90	90	77.756(4)
$\beta$ (°)	75.053(3)	74.468(2)	93.767(3)	106.554(3)	90	66.198(4)
$\gamma$ (°)	86.102(3)	87.240(2)	90	90	90	85.2370(4)
vol (Å <sup>3</sup> )	944.02(10)	971.50(7)	2093.70(17)	2028.82(15)	3422.1(4)	2170.2(3)
<i>D</i> <sub>calcd</sub> (g/cm <sup>3</sup> )	1.465	1.478	1.489	1.278	1.385	1.428
$\mu$ (mm <sup>-1</sup> )	0.213	0.213	0.444	0.190	0.218	0.194
$\theta$ range (°)	1.62 - 26.99	1.58 - 27.0	1.81 - 27.0	1.91 - 27.0	2.05 - 27.00	1.54 - 27.0
<i>Z</i>	2	2	4	4	4	4
range <i>h</i>	-9 to +10	-10 to +10	-9 to +10	-10 to +11	-13 to +14	-15 to +15
range <i>k</i>	-11 to +11	-12 to +12	-21 to +22	-21 to +21	-25 to +18	-17 to +17
range <i>l</i>	-17 to +17	-17 to +17	-18 to +18	-18 to +18	-18 to +18	-18 to +18
reflns collected	11913	20806	24134	45708	15901	32954
independent reflns	4094	4230	4570	4423	3730	9414
obsd reflns	3555	3584	3108	3512	3286	7796
<i>T</i> (K)	296	296	296	296	100	100
<i>R</i> <sub>1</sub>	0.0458	0.0395	0.0418	0.0412	0.0349	0.0357
<i>wR</i> <sub>2</sub>	0.1180	0.1312	0.1025	0.1230	0.0994	0.0990
GOF	1.044	1.176	1.086	0.910	0.812	1.029
CCDC no.	817364	817365	817366	817367	817368	817369

	SFZ/BEN	SFZ/PIC	SFZ/HBEN-T	SFZ/HBEN-M	SFZ/3HNA
chemical formula	C <sub>12</sub> H <sub>14</sub> N <sub>4</sub> O <sub>2</sub> S, C <sub>7</sub> H <sub>7</sub> NO	C <sub>12</sub> H <sub>14</sub> N <sub>4</sub> O <sub>2</sub> S, C <sub>6</sub> H <sub>6</sub> N <sub>2</sub> O	C <sub>12</sub> H <sub>14</sub> N <sub>4</sub> O <sub>2</sub> S, C <sub>7</sub> H <sub>6</sub> NO <sub>2</sub>	C <sub>12</sub> H <sub>14</sub> N <sub>4</sub> O <sub>2</sub> S, C <sub>7</sub> H <sub>7</sub> NO <sub>2</sub>	C <sub>12</sub> H <sub>14</sub> N <sub>4</sub> O <sub>2</sub> S, C <sub>11</sub> H <sub>8</sub> O <sub>3</sub>
formula weight	399.47	400.46	414.46	415.47	466.51
cryst sys	monoclinic	orthorhombic	triclinic	monoclinic	orthorhombic
space group	<i>P</i> 2 <sub>1</sub> / <i>n</i>	<i>Pbca</i>	<i>P</i> $\bar{1}$	<i>P</i> 2 <sub>1</sub>	<i>P</i> 2 <sub>1</sub> 2 <sub>1</sub>
<i>a</i> (Å)	8.4321(7)	9.684(4)	8.3238(6)	8.5398(4)	6.7701(4)
<i>b</i> (Å)	12.9690(11)	15.716(6)	9.5864(8)	18.2753(7)	16.6846(11)
<i>c</i> (Å)	17.5247(16)	25.310(9)	14.0808(11)	13.3498(5)	18.9656(12)
$\alpha$ (°)	90	90	109.249(2)	90	90
$\beta$ (°)	94.200(6)	90	95.432(2)	105.792(2)	90
$\gamma$ (°)	90	90	106.165(2)	90	90
vol (Å <sup>3</sup> )	1911.3(3)	3852(2)	997.06(14)	2004.83(14)	2142.3(2)
<i>D</i> <sub>calcd</sub> (g/cm <sup>3</sup> )	1.388	1.381	1.381	1.376	1.446
$\mu$ (mm <sup>-1</sup> )	0.201	0.201	0.199	0.198	0.196
$\theta$ range (°)	2.33–27.0	3.43–25.80	1.57–27.0	1.59–27.0	2.44–27.0
<i>Z</i>	4	8	2	4	4
range <i>h</i>	-10 to +10	-11 to +11	-10 to +9	-10 to +10	-8 to +2
range <i>k</i>	-16 to +13	-12 to +19	-12 to +12	-23 to +22	-21 to +21
range <i>l</i>	-21 to +22	-30 to +30	-17 to +17	-17 to +17	-23 to +23
reflns collected	15541	23558	15350	20524	10494
independent reflns	4059	3658	4309	7988	4455
obsd reflns	3417	2450	3425	7150	4291
<i>T</i> (K)	296(2)	296(2)	296	296	100(2)
<i>R</i> <sub>1</sub>	0.0860	0.0475	0.0475	0.0365	0.0273
<i>wR</i> <sub>2</sub>	0.2174	0.1094	0.1556	0.0998	0.0805

Table 2. Continued

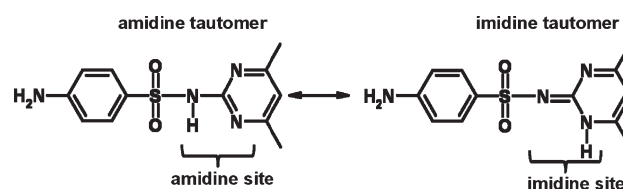
	SFZ/BEN	SFZ/PIC	SFZ/HBEN-T	SFZ/HBEN-M	SFZ/3HNA
GOF	1.059	1.075	0.79	1.202	0.900
CCDC no.	817370	817371	817372	817373	817374

Scheme 2. Synthons Anticipated and/or Observed in the SFZ Co-Crystals<sup>a</sup>

<sup>a</sup> The hydrogen-bonded synthons 11 and 12 are present in the structure of single component (or free) SFZ crystals.

the SFZ molecules. As a result, the molecules form a honeycomb network as shown in Figure 5a,b. Further, the network is doubly interpenetrated as shown in Figure 5c. The disorder modeling of the acetonitrile molecule, from the low temperature (100 K) X-ray data, revealed that the methyl C atom resides on the special position with 50% occupancy factor, while each of the central C and N atoms occupy two separate sites with 50% occupancy factors. The disordered acetonitrile molecule resides between two SFZ pyrimidine rings, resembling a supramolecular cleft (Figure 5d).

**Sulfamethazine/1-Hydroxy-2-naphthoic Acid (1:1) (SFZ/1HNA).** The co-crystal SFZ/1HNA crystallizes in the triclinic  $P\bar{1}$  space group with four molecules in the asymmetric unit. There are two SFZ and two 1HNA molecules in the asymmetric unit in that the molecules in each pair are related by pseudo inversion symmetry. To verify if this occurred due to a wrong unit cell selection, we attempted to solve the structure with a smaller unit cell, with half the size, but the solution was not fruitful. A measurement of the unit cell lengths from the diffraction pattern also supported the selection of the present unit cell. The overlay diagram of the two independent SFZ molecules from the present structure shows that their geometries are slightly different; hence there is no real crystallographic inversion center between them (Figure 6a). This is also evident from the Figure 6b, which shows the mismatch of spatial orientation between the first independent molecule and the inversion related of the second independent molecule. However, the hydrogen bonding patterns of both the independent molecular pairs are very similar. In the crystal structure there are several types of synthons. The 1HNA uses its carboxylic acid group to form synthon 1 with the SFZ molecule as

Scheme 3. Schematic Representation of the Tautomerism in Sulfamethazine Molecule in Some of Its Co-Crystals<sup>a</sup>

<sup>a</sup> Notice the perturbation of aromaticity in pyrimidine ring in the imidine<sub>(SFZ)</sub> tautomer.

the latter exists in its amidine tautomeric form. The hydroxyl group of 1HNA donates its proton for the intramolecular  $O-H \cdots O=C$ , while accepts a hydrogen bond from the SFZ amine group to form  $N-H \cdots O$  (synthon 8). The second proton of the SFZ amine links to the sulfoxy group of another SFZ molecule to form  $N-H \cdots O_{(sulfoxy)}$  (synthon 5). The combination of the hydrogen bonded synthons 1, 5, and 8 between both the co-former molecules result in a double-stranded one-dimensional (1D) linear tape (Figure 6). The adjacent 1D tapes are packed further via weak intermolecular interactions like  $C-H \cdots O_{(sulfoxy)}$ ,  $\pi \cdots \pi$ , and  $C-H \cdots \pi$ .

**Sulfamethazine/Benzamide (1:1) (SFZ/BEN).** The sulfamethazine co-crystallizes with benzamide in monoclinic  $P2_1/n$  space group with one molecule of each SFZ and BEN in the asymmetric unit. In the structure, the SFZ molecule exists in the imidine tautomeric form. Hence, in this case, the SFZ molecule

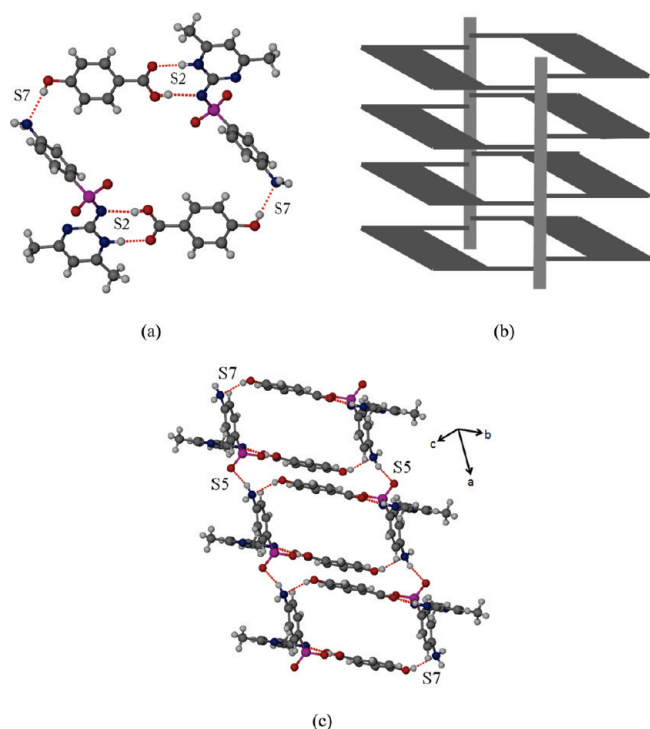


**Figure 1.** (a) A tetramer in the structure of SFZ/HBA formed via synthons 2 (S2) and 7 (S7) by two pairs of SFZ and HBA molecules. (b) A representative model for the two-sided-stepladder. (c) The two-sided stepladder packing of SFZ molecules in the crystal structure where the tetramers are connected via  $N-H \cdots O_{(\text{sulfoxy})}$  synthons (S5) along the  $a$ -axis.

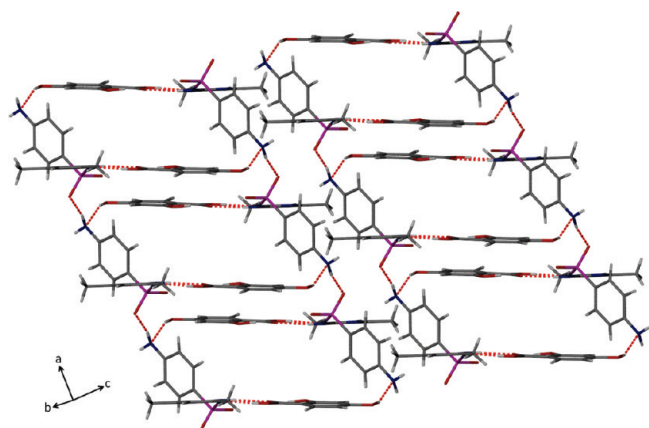


**Figure 2.** Crystal packing in SFZ/DHB. Notice the ladder structure along the  $a$ -axis, similar to that is seen in SFZ/HBA. Adjacent ladders are packed via weak  $C-H \cdots O$  and  $\pi \cdots \pi$  interactions.

offers an imidine site for binding with the BEN amide functional group via synthon 4 ( $N(2)-H(2) \cdots O(3)$ ; 1.93(5) Å, 166(6)°;  $N(5)-H(7B) \cdots N(3)$ ; 2.49(6) Å, 166(5)°). Notably, the  $N-H_{(\text{BEN})} \cdots N_{(\text{sulfonamide})}$  (2.49(6) Å, 166(5)°) in the synthon is significantly weaker than the  $C=O_{(\text{BEN})} \cdots H-N_{(\text{pyrimidine})}$  (1.93(5) Å, 166(6)°). The second proton on the BEN amide  $NH_2$  forms hydrogen bond with the sulfoxy O atom (synthon 9) of an adjacent SFZ molecule. On the other hand, both the acidic amine ( $NH_2$ ) protons of the SFZ molecule involve in two separate

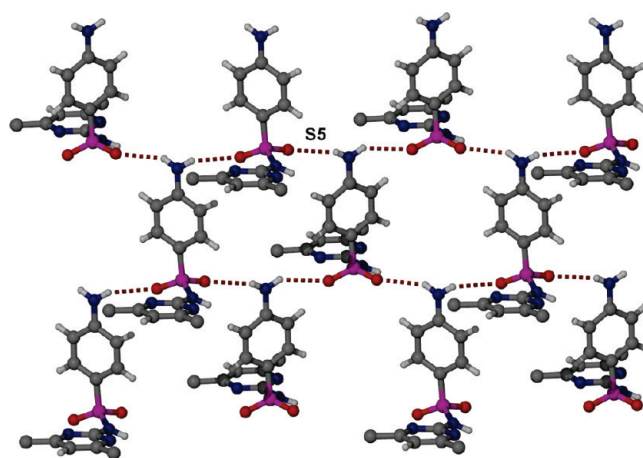


**Figure 3.** Hydrogen bonding pattern in the crystal structure of SFZ/DCB. Formation of synthon 5 (S5) between two SFZ molecules via  $N-H \cdots O=S$  hydrogen bonds, leading to the formation of the 2D square grid network parallel to (010). DCB molecules (that form synthon 1) and methyl hydrogens on pyrimidine ring are not shown for clarity.

$N-H \cdots O_{(\text{sulfoxy})}$  (synthon 5) hydrogen bonds to connect another two adjacent SFZ molecules; as a result each sulfoxy O-atom is also linked to an amine proton. The hydrogen bond leads to a 2D network parallel to the (001) as shown in Figure 7. Because of the V-shape conformation of the SFZ molecule, the alternate pyrimidine rings reach out perpendicular to either side of the 2D sheet. The pyrimidine rings are further stacked with the benzamide aromatic rings to optimize the  $\pi \cdots \pi$  interactions along [100].

**Sulfamethazine/Picolinamide (1:1) (SFZ/PIC).** The SFZ/PIC crystallizes in orthorhombic  $Pbca$  space group with one SFZ molecule and one PIC molecule in the asymmetric unit. The SFZ molecule exists in the imidine tautomeric form to a hydrogen bond to PIC via synthon 4. The two amine hydrogens are involved in two  $N-H \cdots O$  (2.21(3) Å, 159(3)°; 2.31(4) Å, 161(3)°) interactions with the sulfoxy O atoms (synthon 5) of two adjacent SFZ molecules that lead to the formation of 2D hydrogen bonded layers in the (001) as seen in Figure 8b. The packing is further stabilized by the  $\pi \cdots \pi$  interactions between the aromatic rings from both the co-former molecules. The second amide NH of PIC and the second pyrimidine N remain unused in the crystal structure.

**Sulfamethazine/4-Hydroxybenzamide (1:1) (SFZ/HBEN).** The 1:1 co-crystal SFZ/HBEN shows concomitant polymorphism with a triclinic (SFZ/HBEN-T) and a monoclinic (SFZ/HBEN-M) form (Figure 9a). In our initial observations, the crystal morphology of both the forms appeared very similar, but a careful examination revealed that the triclinic crystals are long blocks with four well grown faces, while the monoclinic crystals are thick needles with more than four faces. The triclinic form crystallizes in the  $P\bar{1}$  space group, while the monoclinic form crystallizes in the  $P2_1$  noncentrosymmetric space group. In both forms, the SFZ molecule exists in the imidine tautomeric form to bind to the HBEN molecule via synthon 4 to form a dimer.

In the triclinic form, there is one molecule of each co-former in the asymmetric unit. The SFZ molecule adopts a V-shape conformation in that the two aromatic rings are edge-to-face. The HBEN binds to SFZ via synthon 4 to form a dimer. The dimers are further linked via  $N-H \cdots O_{(\text{sulfoxy})}$  hydrogen bonds

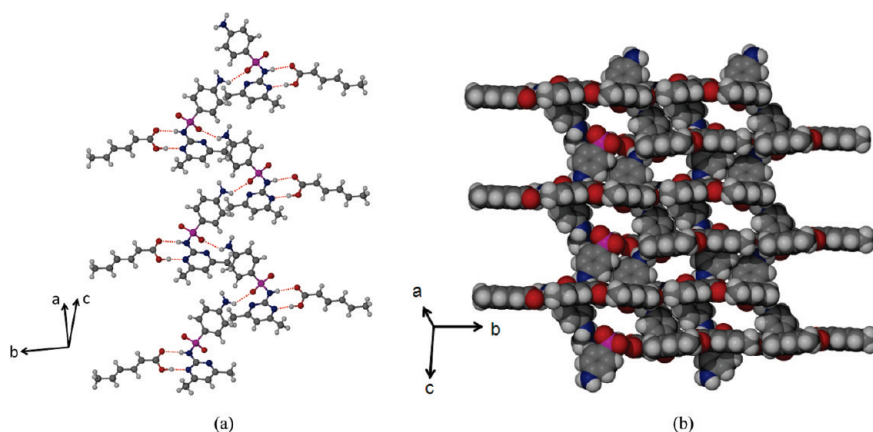


**Figure 4.** Sulfamethazine/sorbic acid (1:1). (a) Packing shows the formation of 2D sheets by SFZ molecules via synthon 5. Notice the interaction of SOR molecules with the SFZ amidine site via synthon 1. (b) Space fill model shows the packing of adjacent 2D ladders.

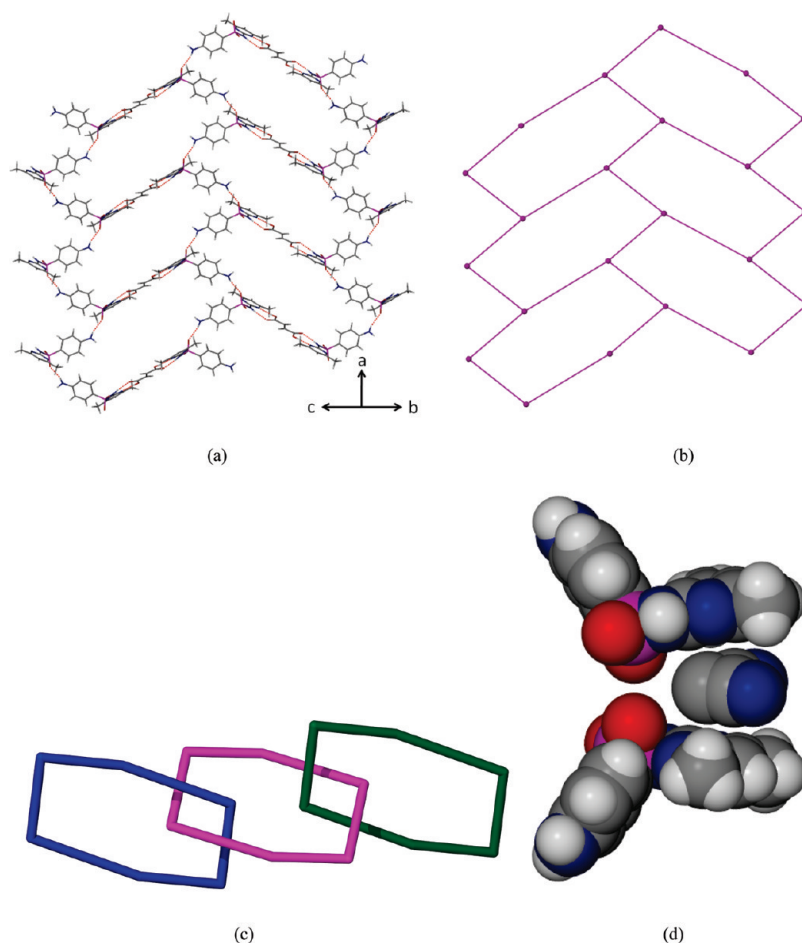


**Figure 5.** Crystal packing in the SFZ/FUM/ACN. (a) The honeycomb network formed by SFZ and FUM molecules via synthons 1 and 4. (b) Honeycomb network that represents packing in (a). (c) Doubly interpenetrated rings from the honeycomb networks. (d) Packing of the disordered acetonitrile molecule between two pyrimidine rings from two SFZ molecules that resemble a supramolecular “cleft”.

(synthon 9) formed by the second proton of the HBEN amide and SFZ sulfoxy groups to make a tetramer (highlighted molecules, Figure 9b). As a result, the SFZ amine and the HBEN hydroxyl groups fall on the same line to involve in a well complemented amino-phenol hydrogen bonded 1D infinite chains along  $[010]$  (Figure 9b).<sup>15</sup> The free lying SFZ amine proton links the sulfoxy O-atom in the  $[101]$  direction.

In the monoclinic form, SFZ/HBEN-M, there are a total of four molecules, with a pair of each co-former, in the asymmetric unit, that is, the molecules in each pair are crystallographically distinct. The two independent SFZ molecules in the structure exist in the imidine tautomeric form and bind to the HBEN molecules via synthon 4. The hydroxyl groups from both the independent HBEN molecules involve in two different hydrogen bond types.

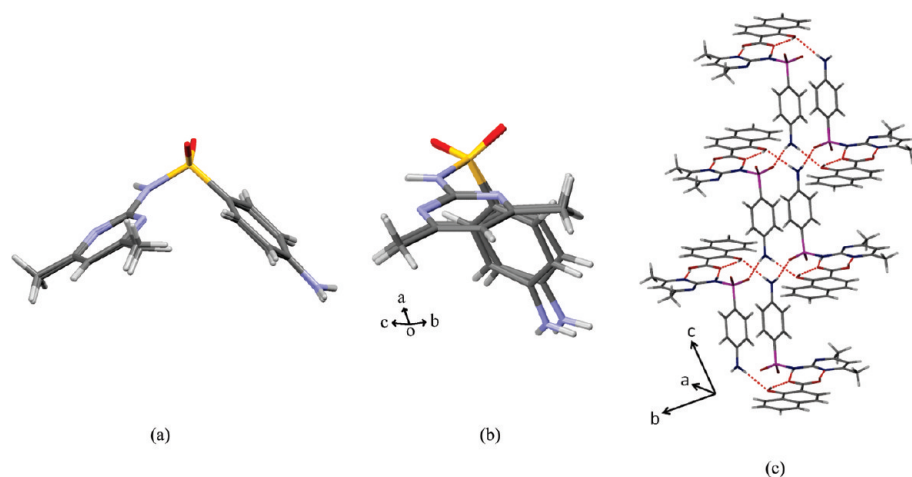


**Figure 6.** Sulfamethazine/1-hydroxy-2-naphthoic acid (1:1). (a) Overlay diagram of the two symmetry independent SFZ molecules to show the conformational differences. (b) The view down along [011] to show the spatial mismatch between two symmetry independent (pseudotranslational related) SFZ molecules from a unit cell. (c) Crystal packing to show the hydrogen bonded synthons 1, 5, and 8 that form the double-stranded 1D linear tape.

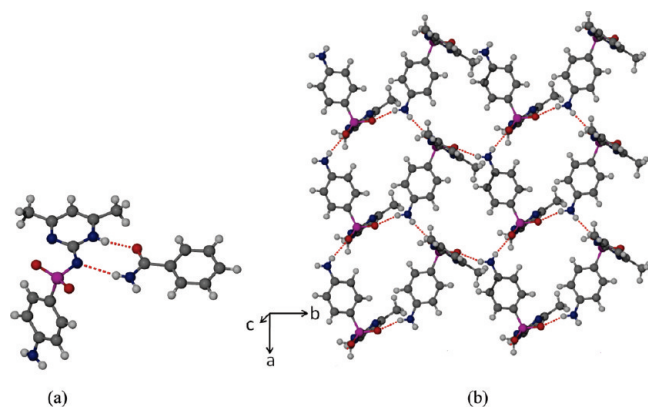


**Figure 7.** Sulfamethazine/benzamide (1:1) co-crystal. (a) Dimer formation between the SFZ imidine tautomer and benzamide via synthon 4. (b) 2D network formed by the SFZ molecules in the structure of co-crystal via  $N-H\cdots O$  (synthon 5) hydrogen bonds between the SFZ amine and sulfoxy groups. The co-former BEN is not shown for clarity.

The first hydroxyl of the pair forms  $O-H\cdots O$  hydrogen bond with the second hydroxyl, while the second hydroxyl links to the SFZ amine group via  $O-H\cdots N$  hydrogen bond (synthon 7). And the amine further donates its two protons to form two  $N-H\cdots O_{(sulfoxy)}$  hydrogen bonds (synthon 5) to link with two different SFZ molecules, all in a co-operative manner (Figure 10). As a result, the amine group from one of the crystallographically independent SFZ is involved in a total of three hydrogen bonds, while the amine group from the other distinct SFZ molecule uses its two protons to make two  $N-H\cdots O_{(sulfoxy)}$  hydrogen bonds, but in this the lone pair of N atom remains unused. Notably, the amine group that utilizes the lone pair adopts a pyramidal shape, while the other remains nearly planar. The hydrogen bond formation among the amine and sulfoxy groups leads to the formation of a honeycomb 2D network parallel to (010) as shown Figure 10a.

**Sulfamethazine/3-Hydroxy-2-naphthoic Acid (1:1) (SFZ/3HNA).** Sulfamethazine and 3-hydroxy-2-naphthoic acid (3HNA)

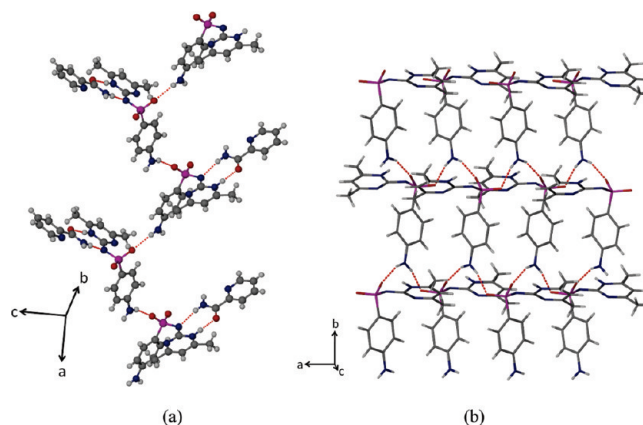
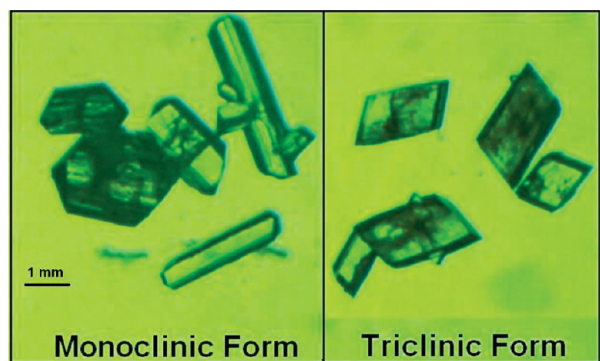
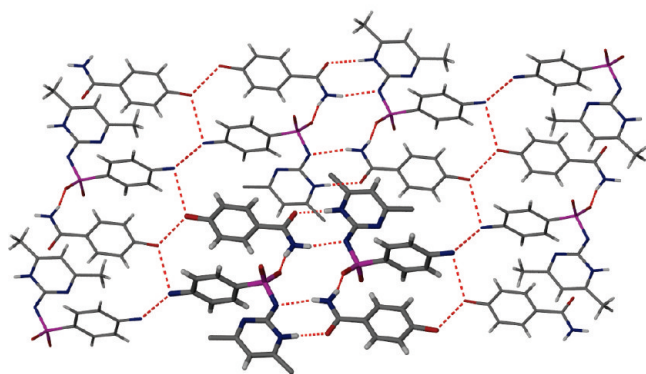


**Figure 8.** Crystal packing in sulfamethazine/picolinamide (1:1). (a) Synthon 4 formation between the SFZ and PIC co-formers and the hydrogen bonds (only one  $N-H\cdots O$  is shown) connecting SFZ molecules via synthon 5. (b) Formation of a 2D network by SFZ molecules via synthon 5 involving both the SFZ amine protons and sulfoxy O atoms.

form a 1:1 co-crystal in the orthorhombic  $P2_12_12_1$  space group. The asymmetric unit consists of one SFZ and one 3HNA molecule. In contrast to the SFZ/carboxylic acid co-crystals, in this structure the SFZ molecule undergoes tautomerism to exist in SFZ imidine form, which is similar to that seen in amide based co-crystals. The carboxylic acid group from 3HNA forms hydrogen bond synthon 2 with the SFZ imidine site. The 3-hydroxyl group of 3HNA involves in an intramolecular  $O-H\cdots O_{(carbonyl)}$  as well as an intermolecular  $N-H\cdots O$  hydrogen bond (synthon 8) with the SFZ amine group that results in a wavelike 1D chain along the crystallographic  $c$ -axis (Figure 11). The second amine hydrogen forms a weak  $N-H\cdots O_{(sulfoxy)}$  ( $2.22(2)$  Å,  $167(2)^\circ$ ) interaction. The adjacent wavelike linear 1D chains pack in a space fill manner along the  $b$ -axis as shown in Figure 11a. The adjacent layers further pack antiparallely to optimize  $\pi\cdots\pi$  interactions along the  $a$ -axis (Figure 11b).



(a)



(b)

**Figure 9.** Sulfamethazine/4-hydroxybenzamide (1:1). (a) Polymorphic crystals of the monoclinic form (SFZ/HBEN-M) and triclinic form (SFZ/HBEN-T). (b) Crystal packing in SFZ/HBEN-T. The tetramer formation (highlighted molecules) via  $S=O \cdots H-N_{(HBEN)}$  (synthon 9) and the infinite amino-phenol hydrogen bonding pattern (synthons 7 and 8) involving the HBEN hydroxyl and SFZ amine groups (protons on O and N atoms are not shown as they could not be refined properly in the structure).

**Density Functional Theory Calculations.** Tautomerism and polymorphism are common phenomena in sulfonamide drugs,<sup>16–19</sup> but the sulfamethazine is not known to show any such phenomena in its single component crystals, in the literature reported thus far.<sup>6</sup> But in all the SFZ/amide co-crystals in this study, the SFZ molecule exists exclusively in the imidine tautomeric form, but never in the amidine tautomeric form. On the contrary, in the SFZ/acid co-crystals, the SFZ exists predominantly in amidine (synthon 1) tautomeric form, except in SFZ/HBA and SFZ/3HNA, where imidine tautomeric form (synthon 2) is involved. To rationalize the SFZ tautomerism in co-crystals, we performed DFT calculations using Gaussian software. The calculations were performed on the free SFZ (1) amidine<sub>(SFZ)</sub> and (2) imidine<sub>(SFZ)</sub> tautomeric forms as well as the hydrogen bonded pairs of the SFZ molecule with (3) benzoic acid (BA), linked via synthon 1, (4) BA linked via synthon 2, (5) benzamide (BEN) linked via synthon 3, (6) BEN linked via synthon 4, (7) 1-hydroxy-2-naphthoic acid (1HNA) linked via synthon 1, (8) 1HNA linked via synthon 2, (9) 3-hydroxy-2-naphthoic acid (3HNA) linked via synthon 1, and (10) 3HNA linked via synthon 2, for estimating the relative energy differences of the two possible synthons in each case. In all the cases, the molecular pairs were taken from corresponding crystal structures and performed geometry optimization, followed by the single point energy

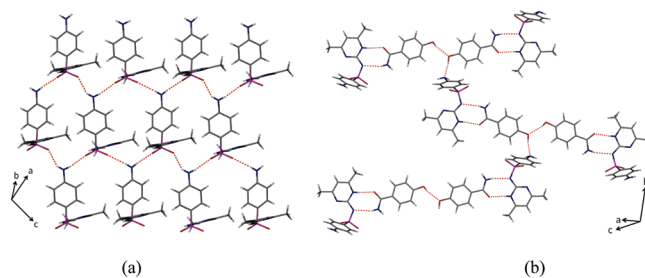


**Figure 10.** Sulfamethazine/4-hydroxybenzamide (1:1) monoclinic form. (a) Crystal packing to show the 2D honeycomb network formed by SFZ molecules via  $N-H \cdots O$  (synthon 5). Notice that the alternate SFZ pyrimidine rings lie above and below perpendicular to the 2D sheet. (b) Linkages of the two SFZ pyrimidine rings from two different 2D sheets by two HBEN molecules. Notice the synthon 7 ( $O-H \cdots N$ ) between the HBEN hydroxyl and SFZ amine groups.

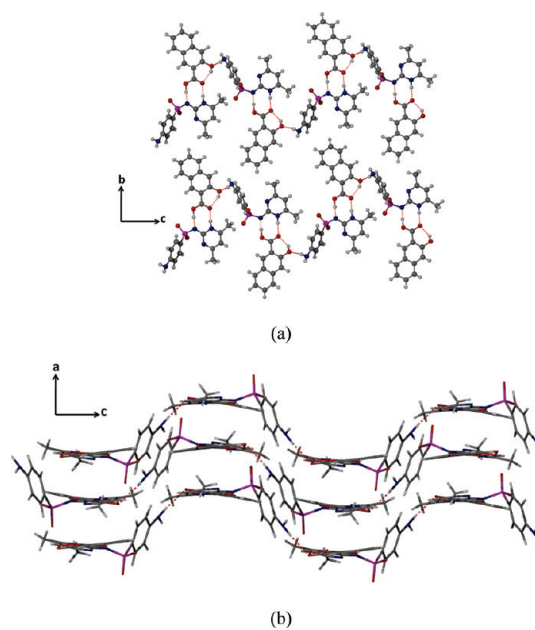


**Figure 11.** Sulfamethazine/3-hydroxy-2-naphthoic acid (1:1), SFZ/3HNA. (a) Crystal packing (view down the *a*-axis) shows the wavelike one-dimensional (1D) chains running along the *c*-axis. (b) Another view (down the *b*-axis) of the 1D chains.

calculations. The energy difference between the amidine and corresponding imidine tautomeric forms of all the calculated molecules are given in Table 3. The calculations reveal that the amidine<sub>(SFZ)</sub> tautomeric form, irrespective of whether hydrogen bonded or free, is more stable than the imidine<sub>(SFZ)</sub> tautomeric form. In case of the free (without co-former) SFZ, the “amidine” tautomer is more stable by 11.43 kcal/mol per molecule than its “imidine” counterpart. The poor stability of the free imidine<sub>(SFZ)</sub> is attributable to the distress caused by the loss of aromaticity at the SFZ pyrimidine ring. However, in the case of the hydrogen bonded SFZ pairs, the energy gap is greatly minimized. For instance, the energies of the amidine<sub>(SFZ)</sub> pairs with both BA (synthon 1) and BEN (synthon 3) are relatively more stable than the imidine<sub>(SFZ)</sub> pairs with BA (synthon 2) and BEN (synthon 4) by 4.39 and 0.63 kcal/mol, respectively. The calculated energies for the amidine<sub>(SFZ)</sub> ··· BA and imidine<sub>(SFZ)</sub> ··· BA pairs show a good

**Table 3. Single Point Energies of the Free Amidine (SFZ), Imidine (SFZ) Tautomers and the Hydrogen Bonded Pairs of SFZ with Some Co-Former Molecules, Obtained from the DFT Calculations**

s. no.	molecular unit(s)	amidine – imidine = energy difference (kcal/mol)
1	amidine <sub>(SFZ)</sub>	
2	imidine <sub>(SFZ)</sub>	11.43
3	amidine <sub>(SFZ)</sub> ··· BA	
4	imidine <sub>(SFZ)</sub> ··· BA	4.39
5	amidine <sub>(SFZ)</sub> ··· BEN	
6	imidine <sub>(SFZ)</sub> ··· BEN	0.63
7	amidine <sub>(SFZ)</sub> ··· 1HNA	
8	imidine <sub>(SFZ)</sub> ··· 1HNA	6.50
9	amidine <sub>(SFZ)</sub> ··· 3HNA	
10	imidine <sub>(SFZ)</sub> ··· 3HNA	1.95

agreement with the fact that the synthon 1 is observed in the previously reported crystal structure of SFZ/BA co-crystal. Similarly, the majority of the studied SFZ/acid co-crystals adopted the synthon 1, except SFZ/HBA and SFZ/3HNA (synthon 2). The contrast behavior of these latter two structures may be understood from the calculations on the amidine/imidine<sub>(SFZ)</sub> hydrogen bonded pairs with 1HNA and 3HNA. In the case of the 1HNA, the energy difference between the amidine<sub>(SFZ)</sub> and imidine<sub>(SFZ)</sub> hydrogen bonded tautomers is 6.5 kcal/mol, while this is only 1.9 kcal/mol in the case of the 3HNA. Hence, as the energy difference in the case of 3HNA pairs is only marginal, the formation of synthon 2 in its crystal structure is understandable.

On the other hand, in all the studied SFZ/amide co-crystals, only the synthon 4, involving the less stable imidine<sub>(SFZ)</sub>, was observed. The calculations showed that the imidine<sub>(SFZ)</sub> ··· BEN pair is only less stable by 0.6 kcal/mol than the amidine<sub>(SFZ)</sub> ··· BEN pair. A careful examination of the geometries of calculated SFZ ··· BEN pairs with synthon 3 and 4 provided some insights. In the amidine<sub>(SFZ)</sub> ··· BEN pair, the synthon 3 was found twisted with a clear puckering of the amide NH<sub>2</sub>(BEN) protons away from the adjacent Me group on the SFZ pyrimidine ring. This suggests a possible high steric repulsion effect on the amide NH<sub>2</sub> protons by the adjacent Me<sub>(SFZ)</sub> group. Hence, the unfavorable secondary interactions such as NH<sub>2</sub>(BEN) ··· Me<sub>(SFZ)</sub> and SO<sub>2</sub>(SFZ) ··· O=C(BEN) seem to deter the formation of synthon 3 in the crystal structures. On the other hand, in the case of synthon 4, the reversal of the amide group on BEN (~180° rotation) leads to favorable SO<sub>2</sub>(SFZ) ··· H<sub>2</sub>N(BEN) and Me<sub>(SFZ)</sub> ··· O=C(BEN) secondary interactions (Figure 12). This was also supported by the presence of stronger hydrogen bonds (smaller matrices) in the calculated synthon 4 than in synthon 3. Here it is to be noted that the small difference of 0.6 kcal/mol in tautomeric SFZ ··· BEN pairs is for the isolated hydrogen bonded molecular pairs with idealized geometries, whereas, in the crystalline state, the molecular geometries are bound to deviate from the idealized positions due to packing constraints; hence the unfavorable or favorable interactions will have a greater influence on the stabilities, and hence the reversal of the relative stabilities for amidine<sub>(SFZ)</sub> and imidine<sub>(SFZ)</sub> tautomeric forms is anticipated. Consideration of similar steric factors is also useful to understand the formation of distinct synthons in the earlier discussed co-crystals of crowded acids, 1HNA (amidine<sub>(SFZ)</sub>);

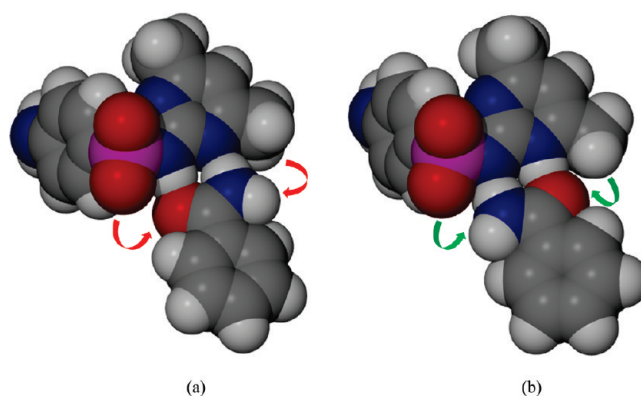


**Figure 12.** The energy optimized molecular pairs of SFZ and BEN bonded via (a) synthon 3 and (b) synthon 4, obtained from Gaussian calculations. (a) The space filling model shows the synthon 3 formation and the unfavorable secondary interactions (red arrows) due to a tight packing of amide NH<sub>2</sub>(BEN) and Me<sub>(SFZ)</sub>, and the SO<sub>2</sub>(SFZ) and O=C(BEN) groups. (b) Synthon 4 formation with favorable secondary interactions (green arrows) between O=C(BEN) ··· Me<sub>(SFZ)</sub> and SO<sub>2</sub>(SFZ) ··· H<sub>2</sub>N(BEN) groups.

synthon 1) and 3HNA (imidine<sub>(SFZ)</sub>; synthon 2). In the case of 3HNA, the formation of synthon 1 (amidine<sub>(SFZ)</sub>) is only less stable by 1.9 kcal/mol than the synthon 2 (imidine<sub>(SFZ)</sub>), while this is 6.5 kcal/mol in the case of 1HNA. Hence, the formation of synthon 2 in SFZ/3HNA is comprehensible as this leads to favorable secondary interactions, as is also the case in SFZ/HBA. Hence, the overall crystal packing and the hydrogen bond preferences of all the functional groups have to be considered for understanding such observations. The studies reveal that this is clearly a case of co-former (or synthon) assisted API tautomerism, where the co-former geometry plays an important role in prompting the tautomerism.

Observation of the tautomerism in SFZ co-crystals inspired us to screen for the new polymorphic forms of the single component SFZ. But, in our quick screening by solvent drop grinding and slow evaporation methods, we did not observe any polymorphism of SFZ. But, it will be no surprise, if a new form of SFZ with imidine tautomeric form is found, as it is clear from these co-crystals that the hydrogen bonding greatly reduces the difference between the amidine and imidine SFZ tautomeric forms. However, this will depend on the possibility of SFZ achieving the stable hydrogen bonded imidine tautomer with minimal steric effects from the pyrimidine methyl group and the sulfoxy O atom.

**Infrared Spectroscopy.** Infrared spectroscopy is a reliable technique to ascertain the formation of co-crystals. Usually co-crystals show the stretching frequency ( $\nu_s$ ) bands of both the co-formers associated with characteristic shifts.<sup>20</sup> For the IR spectroscopy of all the SFZ co-crystals (in the region 400–4000 cm<sup>-1</sup>), two to three single crystals were chosen by inspecting them under an optical microscope. A comparison of the  $\nu_s$  shifts gave an estimate of the relative strengths of the hydrogen bonds formed between the functional groups in co-crystals.<sup>20–24</sup> The detailed peak assignment for the free SFZ and each co-crystal is given in Table 4. In the single component or free SFZ crystals, the stretching frequency band at 3243 cm<sup>-1</sup> is assigned to amidine/imidine NH, while the two bands at 3443 and 3345 cm<sup>-1</sup> are assigned to the *asym* NH<sub>2</sub> and *sym* NH<sub>2</sub> stretching frequencies of amine groups respectively. In the free SFZ crystals, the

Table 4. Infrared Stretching Frequencies for SFZ Amidine NH and Amine NH<sub>2</sub> Groups in Free SFZ and Co-Crystals<sup>a</sup>

peak assignment	SFZ	SFZ/HBA	SFZ/DHB	SFZ/DCB	SFZ/SOR	SFZ/FUM/ACN
amine $\nu(\text{NH}_2)_{\text{asym}}$ ( $\text{cm}^{-1}$ )	3443	3357 (−86)	3379 (−64)	3487 (+44)	3469 (+26)	3478 (+35)
(D···A distance /Å)	3.124	3.104(2)	3.178(2)	3.223(4)	3.182(4)	3.0137(18)
NH···N <sub>(Ar)</sub>						
amine $\nu(\text{NH}_2)_{\text{sym}}$	3345	3293 (−52)	3302 (−43)	3384 (+39)	3370 (+25)	3384 (+39)
sulfonamide $\nu(\text{NH})$	3243	3241 (−2)		3215 (−28)		3250 (+7)
(D···A distance /Å)	2.945	2.756(2)	2.791(2)	2.839(3)	2.830(2)	2.7866(16)
NH···O <sub>(SO<sub>2</sub>)</sub>						

peak assignment	SFZ/1HNA	SFZ/BEN	SFZ/PIC	SFZ/HBEN-T	SFZ/HBEN-M	SFZ/3HNA
amine $\nu(\text{NH}_2)_{\text{asym}}$	3461 (+18)	3435 (−8)	3464 (+21)	3416 (−27)	3435 (−8) 3459 (+16)	3426 (−17)
(D···A distance /Å)	3.0451(18)	2.950(6)	3.186(4)	3.032(3)	2.938(3)	3.0416(19)
amine $\nu(\text{NH}_2)_{\text{sym}}$	3378 (+33)	3352 (+7)	3373 (+28)	3325 (−20)	3332 (−13) 3363 (+18)	3362 (+17)
sulfonamide $\nu(\text{NH})$	3267 (24)	3241 (−2)	3256 (+13)	3194 (−49)	3194 (−49)	3261 (+18)
(D···A distance /Å)	2.8770(18)	2.704(5)	2.762(3)	2.722(3)	2.709(2)	2.7486(18)

<sup>a</sup>The values given in brackets are the frequency shifts in comparison with the corresponding groups in single component SFZ crystals.

amidine NH involves N—H···O<sub>(sulfoxy)</sub> while the amine group involves two N—H···N<sub>(pyrimidine)</sub> hydrogen bonds by utilizing both the protons, whereas, in the co-crystals, the SFZ exists in either amidine or imidine tautomeric form to make hydrogen bonded synthons 1, 2, or 4 with the co-formers; hence the associated stretching bands appear at different frequencies. Similarly, the SFZ amine also involves different synthons (5, 7, 8, or 12) in different co-crystals. The infrared stretching frequencies with the associated shifts (in brackets) in comparison with free SFZ are given in Table 4.

The SFZ/HBA co-crystal shows the stretching frequency bands for both the co-formers with associated shifts confirming the formation of a new phase (Figure 13a). In the co-crystal, the bands for SFZ amine (NH<sub>2</sub>) group are observed at 3357 cm<sup>−1</sup> (*asym* NH<sub>2</sub>) and 3293 cm<sup>−1</sup> (*sym* NH<sub>2</sub>) that have shifts to lower frequencies (−86 and −52 respectively) compared to the free SFZ molecule in its single component crystals. The amidine NH stretching frequency ( $\nu_{\text{NH}}$ ) band, in this case, is not prominent, but a small attributable band is present at 3241 cm<sup>−1</sup> (Figure 13a).

The IR spectra of the polymorphic forms SFZ/HBEN-T and SFZ/HBEN-M are clearly distinct as the stretching frequencies for SFZ imidine NH and amine NH<sub>2</sub> groups in the latter form are split due to a doubling of molecules in the asymmetric unit (Figure 13b). However, the shift of proton from the sulfonamide NH to pyrimidine N atom in the imidine<sub>(SFZ)</sub> did not show any large effect on the stretching frequency of NH compared to the NH in free SFZ, as both the N—H bond distances are close (amidine N—H distance: in free SFZ = 1.069 Å; SFZ/HBEN-T = 0.91(4) Å; SFZ/HBEN-M = 0.91(3) and 0.96(3) Å).

**Thermal Analysis.** A detailed DSC and TGA experiments were carried out for each co-crystal to study the thermal behavior with respect to API. The DSC traces and thermogravimetric data for the sulfamethazine co-crystals are presented in Figures 14 and 15. The DSC thermograms for all the SFZ co-crystals, except SFZ/HBEN and SFZ/FUM/ACN, showed a single endothermic transition corresponding to the melting (Figure 14a). The melting transition temperature of all the co-crystals was distinct from either of the individual components confirming the formation of a new phase. The thermogram in the case of SFZ/HBEN showed two major endotherms at 175.2 and 180 °C (along with a small endotherm at 129.5 °C). A careful separation of the

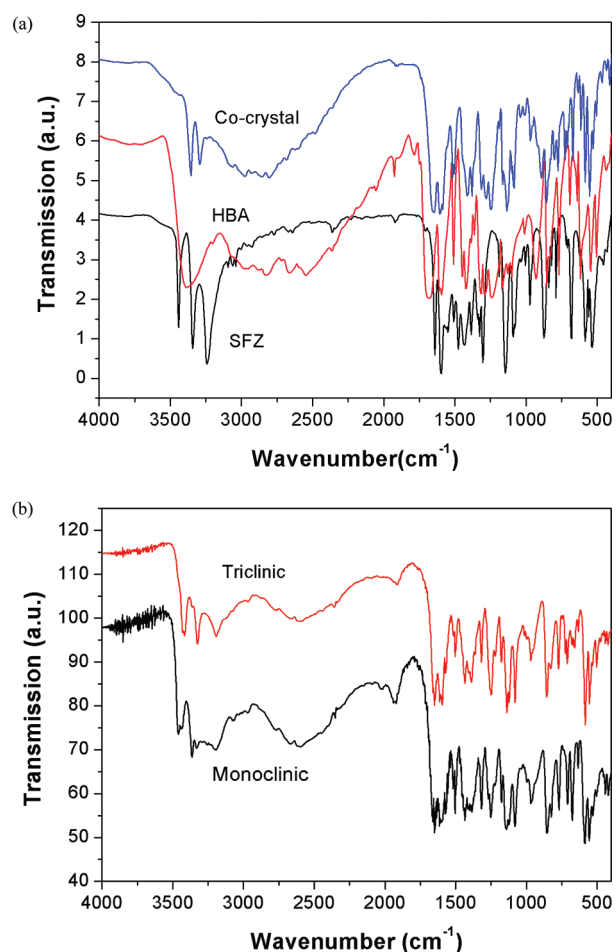
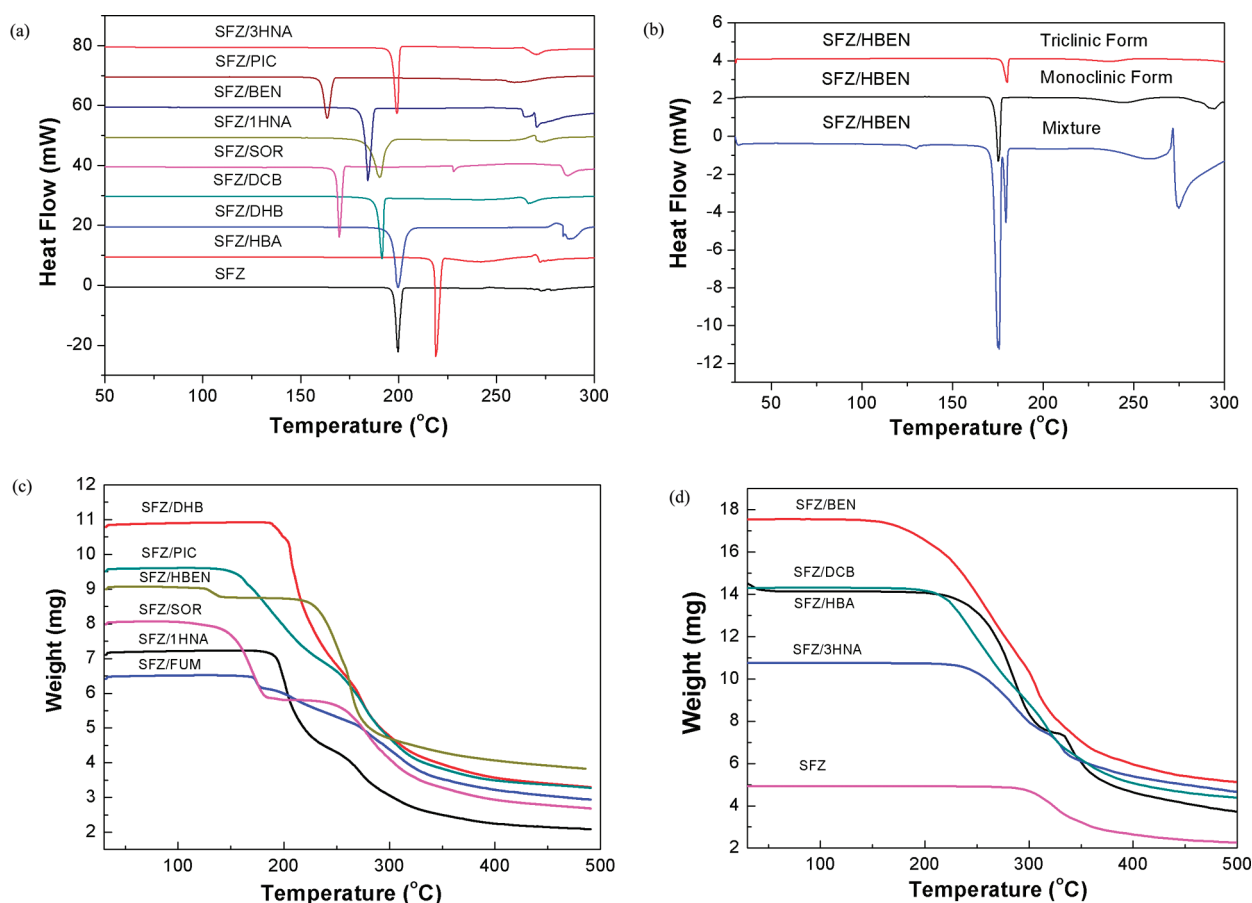


Figure 13. Infrared (IR) spectra of (a) SFZ/HBA and (b) SFZ/HBEN-T and SFZ/HBEN-M forms. Note the splitting of amidine NH and amine NH<sub>2</sub> frequency stretching bands in the SFZ/HBEN-M form due to a pair of symmetry independent SFZ molecules in the asymmetric unit, in (b).

polymorphic crystals using optical microscopy, followed by unit cell determination by SCXRD (using a crystal from each batch)



**Figure 14.** Thermal analysis plots of SFZ co-crystals. (a) DSC of the free SFZ and some SFZ co-crystals, and (b) the SFZ/HBEN polymorphs. Panels (c) and (d) show the TGA plots of all the co-crystals, except SFZ/FUM/ACN.

and then DSC ( $\sim 2$  mg) revealed that the first major endotherm corresponds to the monoclinic form while the second endotherm corresponds to the triclinic form. But the small endotherm at  $129.5^\circ\text{C}$  was not observed in either case, possibly due to the low amount of samples used for the DSC. But the large amounts ( $\sim 10$  mg) of samples taken from two different batches showed a clear proportionate relationship of the small peak to the melting endotherm of the triclinic form. Although it is not a conclusive proof, this suggests to a possible phase transition of the triclinic form to a more stable unknown third form. Further confirmation was not possible as growing triclinic crystals with good yields was difficult.

The co-crystal solvate, SFZ/FUM/ACN, showed three complicated endotherms, with signs of recrystallization, as indicated by the shapes of the last two endotherms in the thermogram (Figure 15a). The TGA experiments confirmed that the first broad endotherm correspond to a loss of solvent ( $\sim 6.2\%$  of the total weight) that matched approximately to one molecule of acetonitrile in the asymmetric unit (Figure 15b). To explicate the second and third endotherms, we carried out DSC and TGA on a sample, which was treated at  $\sim 175^\circ\text{C}$  for 20 min under vacuum followed by cooling to room temperature. The DSC of the resulted solid showed only a single and sharp endotherm exactly at the place of the third endotherm ( $199^\circ\text{C}$ ), which is also same as the mp of the single component SFZ crystalline solid form. The PXRD of the resulted solid confirmed that this is in fact the single component SFZ form. Hence, the other endotherm at  $185^\circ\text{C}$

should correspond to the melting of the co-crystal that is formed/ remained after the solvent loss (Figure 15c). Analysis of the melting endotherms of all the co-crystals reveals that the SFZ/HBA displays an improved thermal stability over the free SFZ crystals, while the DHB and 3HNA co-crystals remain nearly the same and all the remaining co-crystals display decreased thermal stability compared to the API.

**Solubility Studies.** Although we attempted the solubility studies on several co-crystal samples, it was not possible to obtain the estimated values for SFZ co-crystals with SOR, 1HNA, 3HNA, and PIC as both the co-former absorption bands appeared at the same region. In the case of SFZ/BEN ( $0.683\text{ mg/mL}$ ) and SFZ/FUM ( $0.753\text{ mg/mL}$ ), the solubility could be estimated and both showed slightly improved solubility when compared to the free SFZ crystals ( $0.556\text{ mg/mL}$ ).

**Hydrogen Bond Competition.** In the SFZ molecule, there are two types of acceptors and two types of donors with varied strengths. The slightly stronger acceptor,  $\text{O}_{(\text{sulfoxy})}$ , and the weaker acceptors, aromatic ring  $\text{N}_{(\text{pyrimidine})}$  atoms, compete for the strongest amidine donor (NH). In this, the former successfully forms synthon 11, leaving the latter to settle with the next strongest donor, amine ( $\text{NH}_2$ ) to form  $\text{N}-\text{H}\cdots\text{N}$  synthon 12. Notably, the geometrical placement of the amine (para-position) is also a favorable factor for its easy reach to the  $\text{N}_{(\text{pyrimidine})}$  than the sulfonamide NH group. There are no other notable hydrogen bond synthons in the free SFZ structure. But, in the co-crystals, the synthon 11 was never found while synthon 12 was found in

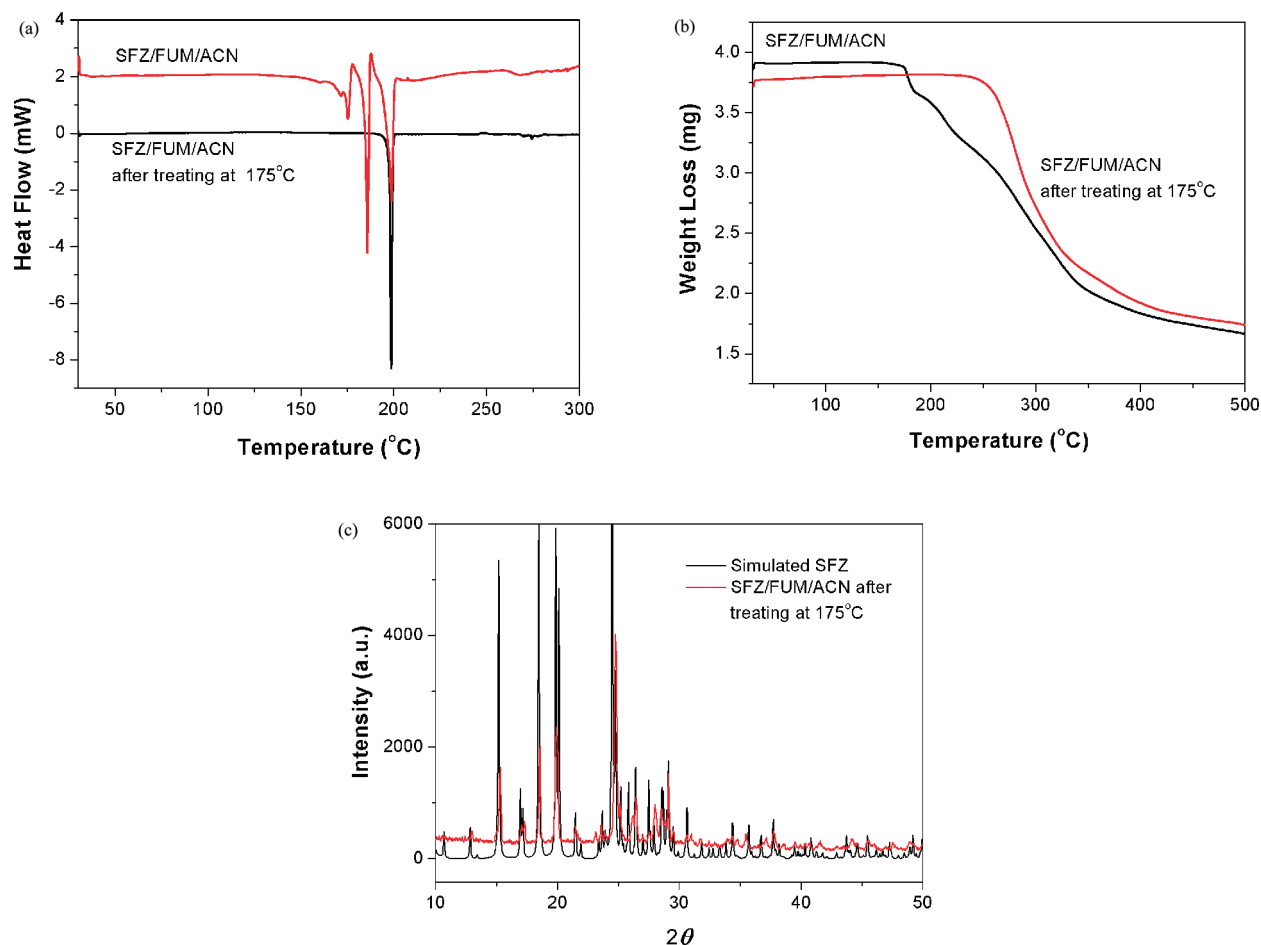


**Figure 15.** (a) DSC plots of the co-crystal solvate, SFZ/FUM/ACN (red) and another batch of sample after treating at 175 °C under a vacuum, and (b) the corresponding TGA plots. (c) The experimental PXR D pattern of the sample treated at 175 °C (red) and the simulated PXR D pattern of the free SFZ (black). Notice the perfect match between the red and black lines.

both SFZ/HBA and SFZ/DHB. The observations are consistent with the fact that a strong donor binds to a strong acceptor and a weak donor to a weak acceptor.<sup>25</sup> In all the co-crystals, the dominant co-former carboxylic acid or amide group primarily binds to the amidine/imidine<sub>(SFZ)</sub> site via synthon 1, 2, or 4. All the amide co-formers interacted with the imidine<sub>(SFZ)</sub> tautomer via synthon 4, but never with amidine<sub>(SFZ)</sub> tautomer via synthon 3, whereas the acid co-formers bind preferentially with the amidine<sub>(SFZ)</sub>, except the HBA and 3HNA which bind by imidine<sub>(SFZ)</sub> tautomer, due to the reasons discussed earlier using the Gaussian calculations.

The remaining SFZ amine and sulfoxy groups are left free to interact either with each other or to compete with the other available hydrogen bonding functional groups from the co-former, if any. When there was no strong competing hydrogen bonding group from the co-former, synthon 5 was always found between the SFZ amine and sulfoxy groups involving both the protons of amine and O atoms of sulfoxy group. Not only that, even when there was a strong competing hydrogen bonding group like OH from the co-former, at least one amine proton and a sulfoxy O atom participated in the synthon 5, in all the cases except in SFZ/HBEN-T. When the co-former had a *p*-OH group (HBA, DHB, HBEN-T, and HBEN-M), in all the cases, the SFZ amine involved additionally in synthon 7 (O–H···N), while when the OH was *ortho*- to the carboxylic acid or amide (where the

OH primarily involved in intramolecular O–H···O<sub>(carbonyl)</sub>), the SFZ amine, instead, formed synthon 8 (N–H···O). The exceptional utilization of all the acceptors and donors is seen in the HBEN-T co-crystal. This could be attributed to the easy accessibility of the OH<sub>(HBEN)</sub> group being at the *para* position. In the structure, the complementary amino-phenol synthons 7 and 8 are present, alongside the rare synthons 9 and 10 in this study. Synthon 9 is also found in the SFZ/BEN. Analysis of the other SFZ co-crystals reported in the literature also showed a very similar hydrogen bonding pattern.

**Conclusion.** In conclusion, 10 new SFZ co-crystals with carboxylic acids and amides are synthesized and characterized thoroughly by single crystal XRD, DSC, TGA, and infrared spectroscopy. DSC and TGA was used to confirm the relative stabilities of the new solid forms compared to the free SFZ. Sulfamethazine shows co-former induced amidine-imidine tautomerism in co-crystals. The acid co-crystals bind to the SFZ via synthon 1 or 2, while the amides bind via synthon 4, but never via synthon 3. This is because the formation of synthon 3 is sterically hindered due to repulsion between the pyrimidine methyl group of SFZ and the co-former amide NH<sub>2</sub> group, as well as the unfavorable repulsion between the sulfoxy O atoms and the amide carbonyl O atom from the co-former, whereas such steric hindrance is absent in case of synthon 4 formation, though there

is a loss of aromatic energy on the SFZ pyrimidine ring of the imidine<sub>(SFZ)</sub>, which is again made up by the hydrogen bond formation energy. The geometry and hydrogen bonding functional groups on the co-formers are shown to influence the type of synthons formed by the SFZ sulfonamide and amine groups in the co-crystals. The hydrogen bond synthons observed in the structures are consistent with the fact that the strong acceptors prefer strong donors and the weak acceptors prefer the weak donors.

## ■ ASSOCIATED CONTENT

**S Supporting Information.** Geometrical parameters of significant hydrogen bonds in all the co-crystals (Table S1); ORTEP diagrams (Figures S1–S10); powder X-ray diffraction patterns of bulk co-crystal samples (Figures S11 and S12); IR spectral data of the co-crystals (Figure S13–S21); Crystallographic information files (CIFs). This material is available free of charge via the Internet at <http://pubs.acs.org>.

## ■ AUTHOR INFORMATION

### Corresponding Author

\*E-mail: [cmallareddy@rediffmail.com](mailto:cmallareddy@rediffmail.com).

## ■ ACKNOWLEDGMENT

S.G. thanks the CSIR (New Delhi) for JRF. P.P.B. thanks the CSIR for SRF. C.M.R. thanks the DST (SR/FT/CS-074/2009) for funding. We thank Dr. Sanjio S. Zade (IISER Kolkata) for his suggestions and help with the DFT calculations.

## ■ REFERENCES

- (1) (a) Desiraju, G. R. *Crystal Engineering: The Design of Organic Solids*; Elsevier: New York, 1989. (b) Desiraju, G. R. *Angew. Chem., Int. Ed.* **2007**, *46*, 8342–8356. (c) *Frontiers in Crystal Engineering*; Tiekink, E., Vittal, J. J., Eds.; Wiley: Chichester, U. K., 2006.
- (2) (a) Trask, A. V.; Motherwell, W. D. S.; Jones, W. *Cryst. Growth Des.* **2005**, *5*, 1013–1021. (b) Almarsson, Ö.; Zaworotko, M. J. *Chem. Commun.* **2004**, 1889–1896. (c) Vishweshwar, P.; McMahon, J. A.; Bis, J. A.; Zaworotko, M. J. *J. Pharm. Sci.* **2006**, *95*, 499–516. (d) Vishweshwar, P.; McMahon, J. A.; Oliveira, M.; Peterson, M. L.; Zaworotko, M. J. *J. Am. Chem. Soc.* **2005**, *125*, 16802–16803. (e) Thakuria, R.; Nangia, A. *CrystEngComm* **2011**, *13*, 1759–1764.
- (3) (a) Good, D. J.; Rodríguez-Hornedo, N. *Cryst. Growth Des.* **2009**, *9*, 2252–2264. (b) NcNamara, D. P.; Childs, S. L.; Giordano, J.; Iarriccio, A.; Cassidy, J.; Shet, M. S.; Mannion, R.; O'Donnell, E.; Park, A. *Pharm. Res.* **2006**, *23*, 1888–1897. (c) Sun, C. C.; Hou, H. *Cryst. Growth Des.* **2008**, *8*, 1575–1579. (d) Chattoraj, S.; Shi, L.; Sun, C. C. *CrystEngComm* **2010**, *12*, 2466–2472. (e) Karki, S.; Frišćić, T.; Fábíán, L.; Laity, P. R.; Day, G. M.; Jones, W. *Adv. Mater.* **2009**, *21*, 3905–3909. (f) Reddy, C. M.; Padmanabhan, K. A.; Desiraju, G. R. *Cryst. Growth Des.* **2006**, *6*, 2720–2731. (g) Reddy, C. M.; Kirchner, M. T.; Gundakaram, R. C.; Desiraju, G. R. *Chem.—Eur. J.* **2006**, *12*, 2222–2234. (h) Reddy, C. M.; Krishna, G. R.; Ghosh, S. *CrystEngComm* **2010**, 2296–2314.
- (4) (a) Nangia, A.; Desiraju, G. R. *Top. Curr. Chem.* **1998**, *198*, 57. (b) Desiraju, G. R. *Angew. Chem., Int. Ed. Engl.* **1995**, *34*, 2311. (c) Parveen, S.; Davey, R. J.; Dent, G.; Pritchard, R. G. *Chem. Commun.* **2005**, 1531. (d) Florence, A. J.; Shankland, K.; Gelbrich, T.; Hursthouse, M. B.; Shankland, N.; Johnston, A.; Fernandes, P.; Leec, C. K. *CrystEngComm* **2008**, *10*, 26. (e) Takasuka, M.; Nakai, H.; Shiro, M. *J. Chem. Soc., Perkin Trans.* **1982**, *2*, 1061. (f) Thakur, T. S.; Desiraju, G. R. *Cryst. Growth Des.* **2008**, *8*, 4031–4044.
- (5) (a) Desiraju, G. R.; Steiner, T. *The Weak Hydrogen Bond in Structural Chemistry and Biology*; Oxford University Press, Oxford, UK, 1999. (b) Steiner, T. *Acta Crystallogr.* **2001**, *B57*, 103–106. (c) Huang, C. Y.; Cabell, L. A.; Lynch, V.; Anslyn, E. V. *J. Am. Chem. Soc.* **1992**, *114*, 1900–1901. (d) Adson, D. A.; Grant, D. J. W. *J. Pharm. Sci.* **2001**, *90*, 2058–2077. (e) Reddy, L. S.; Chandran, S. K.; George, S.; Babu, N. J.; Nangia, A. *Cryst. Growth Des.* **2009**, *7*, 2675–2690. (f) Sarma, B.; Nath, N. K.; Bhogala, B. R.; Nangia, A. *Cryst. Growth Des.* **2009**, *9*, 1546–1557.
- (6) (a) Tiwari, R. K.; Haridas, M.; Singh, T. P. *Acta Crystallogr.* **1984**, *C40*, 655. (b) Maury, L.; Rambau, J.; Pauvert, B.; Lasserre, Y.; Bergé, G.; Audran, M. *J. Pharm. Sci.* **1985**, *74*, 422–426.
- (7) (a) McIntosh, J. M.; Robinson, R. H. M.; Selbie, F. R.; Reidy, J. P.; Elliott Blake, H.; Guttman, L. *Lancet* **1945**, *246*, 97–99. (b) Giuseppetti, G.; Tadini, C.; Bettinetti, G. P. *Acta Crystallogr.* **1994**, *C50*, 1289–1291. (c) Nakai, H.; Takasuka, M.; Shiro, M. *J. Chem. Soc., Perkin Trans. 2* **1984**, 1459–1464.
- (8) (a) Caira, M. R. *Mol. Pharmaceutics* **2007**, *4*, 310–316. (b) Caira, M. R. *J. Chem. Crystallogr.* **1994**, *24*, 695–701. (c) Caira, M. R. *J. Crystallogr. Spectrosc. Res.* **1992**, *22*, 193–200. (d) Caira, M. R.; Bettinetti, G.; Sorrenti, M.; Catenacci, L. *J. Pharm. Sci.* **2003**, *92*, 2164–2176. (e) Lu, J.; Rohani, S. *J. Pharm. Sci.* **2010**, *99*, 4042–4047. (f) Patel, U.; Haridas, M.; Singh, T. P. *Acta Crystallogr.* **1988**, *C44*, 1264–1267. (g) Sardone, N.; Bettinetti, G.; Sorrenti, M. *Acta Crystallogr.* **1997**, *C53*, 1295–1299. (h) Ghose, S.; Chakrabarti, C.; Dattagupta, J. K. *Acta Crystallogr.* **1988**, *C44*, 1810–1813.
- (9) (a) SAINT Plus (version 6.45); Bruker AXS Inc.: Madison, WI, 2003. (b) SMART (version 5.625) and SHELX-TL (version 6.12); Bruker AXS Inc.: Madison, WI, 2000.
- (10) Barbour, L. J. *X-Seed, Graphical Interface to SHELX-97 and POV-Ray*; University of Missouri; Columbia: Columbia, MO, 1999.
- (11) Basavoju, S.; Boström, D.; Velaga, S. P. *Cryst. Growth Des.* **2006**, *6*, 2699–2708.
- (12) Frisch, M. J.; Trucks, G. W.; Schlegel, H. B.; Scuseria, G. E.; Robb, M. A.; Cheeseman, J. R.; Montgomery, J. A., Vreven, T.; Kudin, K. N.; Burant, J. C.; Millam, J. M.; Iyengar, S. S.; Tomasi, J.; Barone, V.; Mennucci, B.; Cossi, M.; Scalmani, G.; Rega, N.; Petersson, G. A.; Nakatsuji, H.; Hada, M.; Ehara, M.; Toyota, K.; Fukuda, R.; Hasegawa, J.; Ishida, M.; Nakajima, T.; Honda, Y.; Kitao, O.; Nakai, H.; Klene, M.; Li, X.; Knox, J. E.; Hratchian, H. P.; Cross, J. B.; Bakken, V.; Adamo, C.; Jaramillo, J.; Gomperts, R.; Stratmann, R. E.; Yazyev, O.; Austin, A. J.; Cammi, R.; Pomelli, C.; Ochterski, J. W.; Ayala, P. Y.; Morokuma, K.; Voth, G. A.; Salvador, P.; Dannenberg, J. J.; Zakrzewski, V. G.; Dapprich, S.; Daniels, A. D.; Strain, M. C.; Farkas, O.; Malick, D. K.; Rabuck, A. D.; Raghavachari, K.; Foresman, J. B.; Ortiz, J. V.; Cui, Q.; Baboul, A. G.; Clifford, S.; Cioslowski, J.; Stefanov, B.; Liu, G.; Liashenko, A.; Piskorz, P.; Komaromi, I.; Martin, R. L.; Fox, D. J.; Keith, T.; Al-Laham, M. A.; Peng, C. Y.; Nanayakkara, A.; Challacombe, M.; Gill, P. M. W.; Johnson, B.; Chen, W.; Wong, M. W.; Gonzalez, C.; Pople, J. A. *Gaussian 03*, revision E. 01, Wallingford CT: Gaussian, Inc. 2004.
- (13) (a) Becke, A. D. *J. Chem. Phys.* **1993**, *98*, 5648–5652. (b) Lee, C.; Yang, W.; Parr, R. G. *Phys. Rev. B* **1988**, *37*, 785–789.
- (14) (a) Hehre, W. J.; Ditchfield, R.; Pople, J. A. *J. Chem. Phys.* **1972**, *56*, 2257–2261. (b) Hariharan, P. C.; Pople, J. A. *Theor. Chem. Acta* **1973**, *28*, 213–222.
- (15) Vangala, V. R.; Bhogala, B. R.; Dey, A.; Desiraju, G. R.; Broder, C. K.; Smith, P. S.; Mondal, R.; Howard, J. A. K.; Wilson, C. C. *J. Am. Chem. Soc.* **2003**, *125*, 14495–14509.
- (16) (a) Yang, S. S.; Guillory, J. K. *J. Pharm. Sci.* **1972**, *61*, 26–40. (b) Bernstein, J.; Davis, R. E.; Shimoni, L.; Chang, N. L. *Angew. Chem., Int. Ed. Engl.* **1995**, *34*, 1555. (c) Etter, M. C.; Macdonald, J. C. *Acta Crystallogr.* **1990**, *B46*, 256. (d) Grell, J.; Bernstein, J.; Tinhofer, G. *Acta Crystallogr.* **1999**, *B55*, 1030.
- (17) (a) Kitaigorodskii, A. I. *Molecular Crystals and Molecules*; Academic Press: New York, 1973. (b) Desiraju, G. R.; Sarma, J. A. R. *Proc. Ind. Acad. Sci. (Chem. Sci.)* **1986**, *96*, 599.
- (18) Gelbrich, T.; Threlfall, T. L.; Bingham, A. L.; Hursthouse, M. B. *Acta Crystallogr.* **2007**, *C63*, o323–o326.
- (19) Jetti, R. K. R.; Boese, R.; Sarma, J. A. R. P.; Reddy, L. S.; Vishweshwar, P.; Desiraju, G. R. *Angew. Chem., Int. Ed.* **2003**, *42*, 1963–1967.
- (20) Sanphui, P.; Sarma, B.; Nangia, A. *Cryst. Growth Des.* **2010**, *10*, 4550–4564.

- (21) Gelbrich, T.; Threlfall, T. L.; Bingham, A. L.; Hursthouse, M. B. *Acta Crystallogr.* **2007**, C63, o323–o326.
- (22) Kesimli, B.; Topaçli, A.; Topaçli, C. *J. Mol. Struct.* **2003**, 645, 199–204.
- (23) Hossain, G. M.; Amoroso, A. J.; Banu, A.; Malik, K. M. A. *Polyhedron* **2007**, 26, 967–974.
- (24) Nakai, H.; Takasuka, M. *Vib. Spectrosc.* **2001**, 25, 197–204.
- (25) Etter, M. C. *Acc. Chem. Res.* **1990**, 23, 120–126.